CRYSTAL GROWTH & DESIGN

Article

pubs.acs.org/crystal

Polymorphs and Solvates of 2-(1,4-Dihydro-1,4-dioxonaphthalen-3-ylthio)benzoic Acid

Bigyan R. Jali and Jubaraj B. Baruah*

Department of Chemistry, Indian Institute of Technology Guwahati, Guwahati 781 039, Assam, India

Supporting Information

ABSTRACT: Three conformational polymorphs of 2-(1,4-dihydro-1,4-dioxonaphthalen-3-ylthio) benzoic acid (**L**), an acetonitrile solvate of **L**, and cocrystal of **L** with 2,2′-bipyridine are structurally characterized. The two polymorphs **I** and **II** have $Z' = 1$ and possess $R_2^2(8)$ type of dimeric structure in which the two aromatic rings are in trans disposition across the cyclic hydrogen bonded motifs. However, the dihedral angles between the aromatic ring and 2-methyl 1,4-naphthoquinone rings are −129.38° and 126.56°, respectively. The polymorph **III** has $Z' = 2$; it shows $R_2^2(8)$ type of dimeric structures which are formed by two symmetry independent molecules. In its crystal lattice, the aromatic rings across the cyclic hydrogen bond motifs are in cis dispositions. Dihedral angles between the aromatic ring and 2-methyl 1,4-naphthoquinone ring in the two symmetry independent molecules are 114.82° and 125.27°, respectively. The acetonitrile solvate of **1** has $Z' = 3$. In its crystal lattice, it has two symmetry independent molecules forming $R_2^2(8)$ hydrogen bonds to form dimeric assemblies and another cyclic $R_2^2(8)$ type hydrogen bond geometry between molecules which constitute the third set of symmetry independent molecules. The 2-(1,4-dihydro-1,4-dioxonaphthalen-3-ylthio)benzoic acid also forms a 2:1 cocrystal with 2,2′-bipyridine; in this cocrystal the two nitrogen atoms are trans to each other and they participate in hydrogen bonds with carboxylic acids.

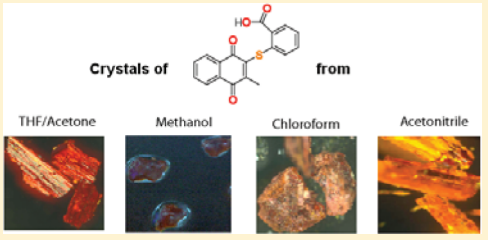

INTRODUCTION

Polymorphism is the existence of the same chemical composition in more than one crystalline modification, and solvates refer to the cases in which the same given substance includes solvent during crystallization.[1] The necessities to design crystalline solids with desired structures and properties led to great progress in the study of polymorphism.[2] Controlling the formation of a specific polymorph is a challenge[3] in crystal engineering. The solvents have an important role in the preparation of polymorphs.[4] Polymorphism tends to be prominent in molecules that have multiple options for hydrogen bond formation,[5] which is reflected in a number of active pharmaceutical ingredients.[6]

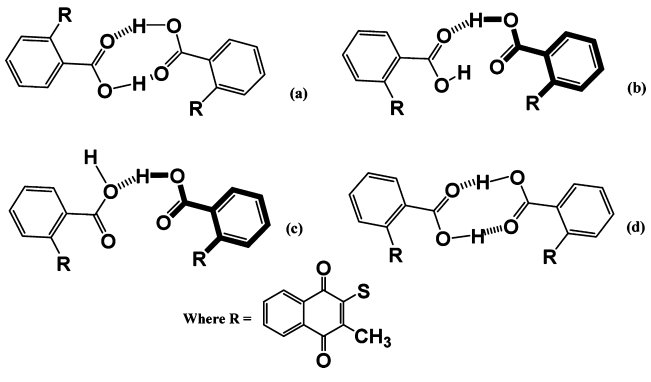

Figure 1. (a–d) Some dimeric hydrogen bonded motifs of carboxylic acid.

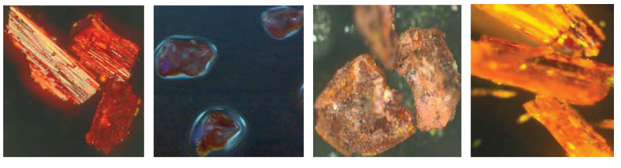

Figure 2. The crystal morphology of polymorphs **I**–**III** and acetonitrile solvate **IV**.

We have shown that the packing pattern guided by weak C–H···O interactions helps in the formation of different motifs in sulfur-containing quinone compounds.[7] Quinone compounds having thiolate groups show conformational polymorphism.[8] But because of subtle energy differences among the polymorphic structures only stable ones are generally isolated.[7a] Conformational polymorphs in quinonic type compounds such as fuchsones are well documented, but the approach has not been extended to quinones.[9] Thus, we felt that introduction of a functional group such as carboxylic acid capable of forming hydrogen bonds in different ways may help in getting more numbers of stable conformational polymorphs. Carboxylic acids generally adopt the $R^2_2(8)$ type[10] of cyclic structure; puckering of such structural motifs may lead to other orientations (Figure 1),

Received: March 7, 2012
Revised: May 2, 2012
Published: May 8, 2012

   dx.doi.org/10.1021/cg300318u | *Cryst. Growth Des.* 2012, 12, 3114–3122

Scheme 1. Different Polymorphs, Solvates, and Cocrystals of L

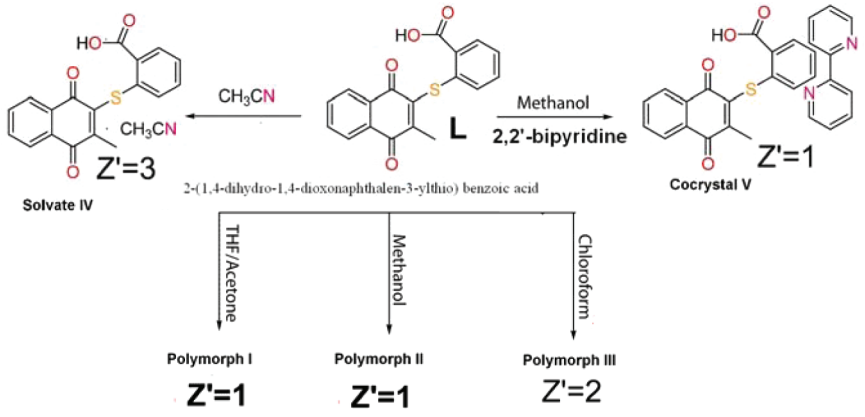

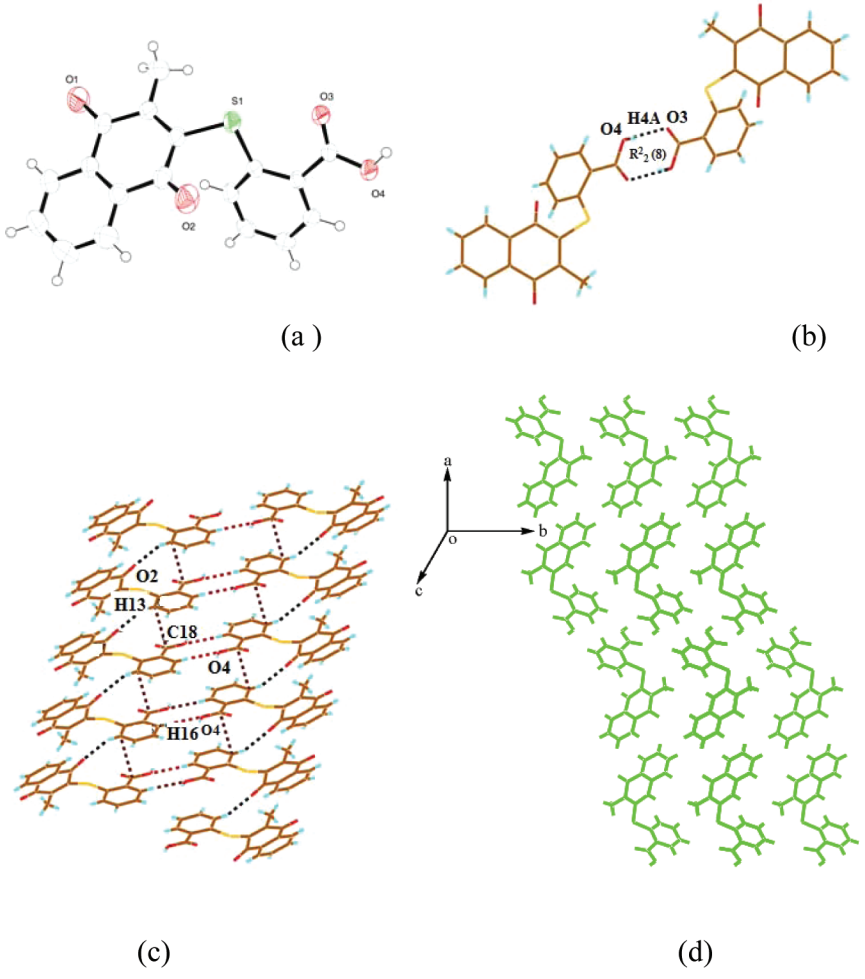

Figure 3. (a) ORTEP diagram of polymorph **I** drawn with 50% thermal ellipsoids. (b) Cyclic H-bonding motif. (c) C−H···O and π-interactions in polymorph **I**. (d) The packing diagram *a*-crystallographic axis.

which may be stabilized by the hydrogen bond interactions of the carbonyl groups of quinone.

Further to these, the study of the structural aspects of 2-methyl-naphthoquinone derivative such as **L** (Scheme 1) would throw light on the assembling properties of thiosalicylic acid derivatives that are used as active pharmaceutical ingredients.[11] Moreover, the 2-methyl-napthoquinone part attached to the thiosalicylic acid has some structural similarities to vitamin K, and some of these compounds show interesting polymorphic structures.[12] Thus, a 2-methyl-naphthoquinone unit attached to a thiosalicylic acid part can be considered as a model compound of medicine, in which a part having nutrient value is attached to a medicinal component. With these points in mind, we have synthesized a 2-methyl 1,4-naphthoquinone functionalized carboxylic acid 2-(1,4-dihydro-1,4-dioxonaphthalen-3-ylthio)benzoic acid (**L**) to study its polymorphs. During our systematic investigation, we have obtained three conformational polymorphs (**I**, **II**, and **III**), one acetonitrile solvate (**IV**), and one cocrystal (**V**) with 2,2′-bipyridine of **L** as shown in Scheme 1. The structural study of all these polymorphs is demonstrated.

dx.doi.org/10.1021/cg300318u | *Cryst. Growth Des.* 2012, 12, 3114−3122

Table 1. Hydrogen Bond Parameters (Å, °) for Polymorphs I, II, III

polymorph	D−H···A	d_{D-H}	$d_{H\cdots A}$	$d_{D\cdots A}$	∠D−H···A
I	O4−H4A···O3 [3 − *x*, 2 − *y*, −*z*]	0.82	1.84	2.66 (2)	173.4
	C11−H11C···S1	0.96	2.69	3.14 (3)	109.2
	C13−H13···O2 [−1 + *x*, *y*, *z*]	0.93	2.44	3.29 (3)	152.5
	C16−H16···O4	0.93	2.36	2.70 (3)	132.2
II	O4−H4A···O3 [3 − *x*, 2 − *y*, −*z*]	0.82	1.84	2.64 (10)	168.0
	C11−H11A···S1	0.96	2.77	3.08 (10)	100.1
	C11−H11B···O1	0.96	2.38	2.81 (12)	107.0
	C16−H16···O1 [1 + *x*, 1 + *y*, *z*]	0.93	2.48	3.13 (12)	127.4
	C16−H16···O4	0.93	2.40	2.73 (12)	101.0
III	O3−H31···O7 [2 − *x*, 1/2 + *y*, 1/2 − *z*]	0.82	1.82	2.63 (3)	175.4
	O8−H8···O4 [2 − *x*, −1/2 + *y*, 1/2 − *z*]	0.82	1.81	2.62 (3)	171.5
	C2−H2···O4 [1 − *x*, −1/2 + *y*, 1/2 − *z*]	0.93	2.58	3.30 (5)	134.9
	C3−H3···O6 [−1/2 − *x*, −*y*, −1/2 + *z*]	0.93	2.56	3.17 (5)	123.8
	C4−H4···O6	0.93	2.57	3.18 (5)	123.2
	C11−H11A···S1	0.96	2.77	3.12 (4)	103.0
	C11−H11B···O1	0.96	2.36	2.74 (5)	103.0
	C13−H13···O2 [−1 + *x*, *y*, *z*]	0.93	2.58	3.37 (4)	143.8
	C20−H20···O5	0.93	2.66	3.19	116.9

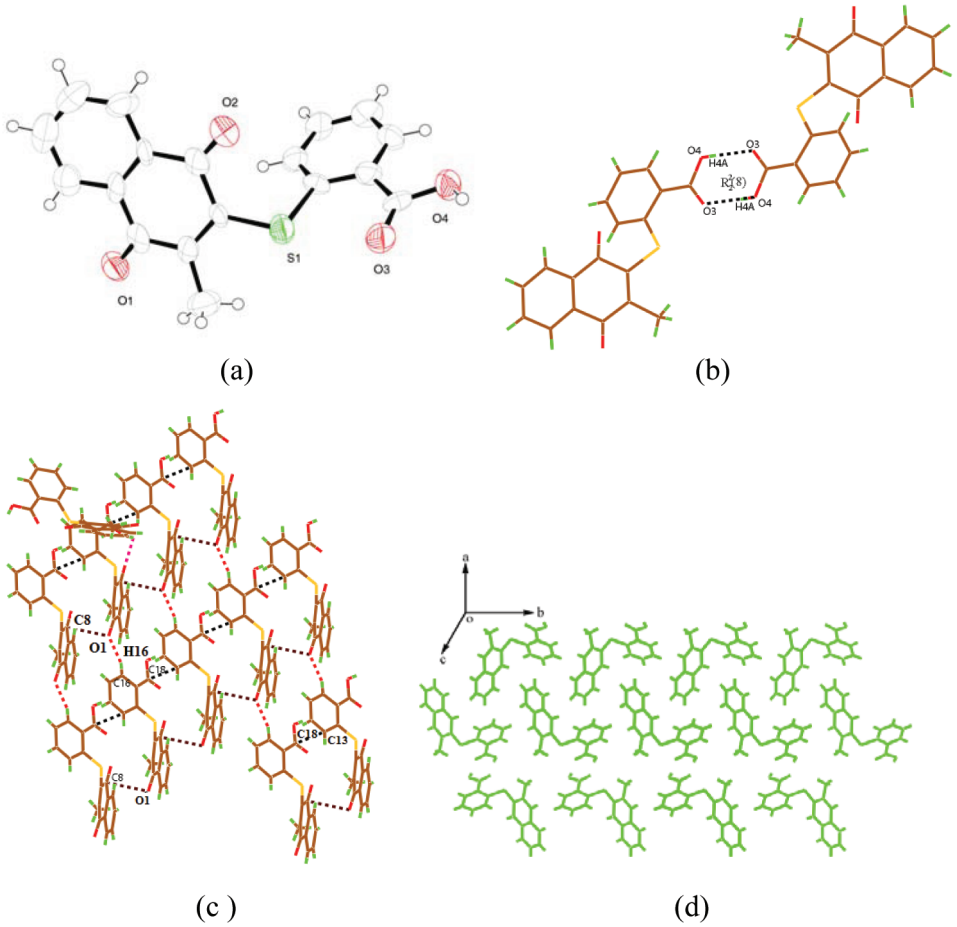

Figure 4. (a) Structure polymorph **II** (50% thermal ellipsoids). (b) Dimeric H-bond motif. (c) Selected C−H···O, C−H···π interactions. (d) Packing diagram of **II**.

RESULTS AND DISCUSSION

The 2-(1,4-dihydro-1,4-dioxonaphthalen-3-ylthio)benzoic acid (**L**) was prepared by coupling of the 2-methyl 1,4-napthoquinone with thiosalicylic acid in aerial condition. The reaction passes through formation of 1,4-dihydroxy naphthalene derivative which gets quickly oxidized under ambient conditions. Such coupling reactions directly leading to substituted naphthoquinones are well documented in the literature.[13] As illustrated in Scheme 1 from compound **L** we could obtain three polymorphs **I**−**III** in unsolvated form and its acetonitrile solvate. The crystal morphology of each polymorph is different and the optical micrographs showing their crystal morphology are shown in Figure 2.

dx.doi.org/10.1021/cg300318u | *Cryst. Growth Des.* 2012, 12, 3114−3122

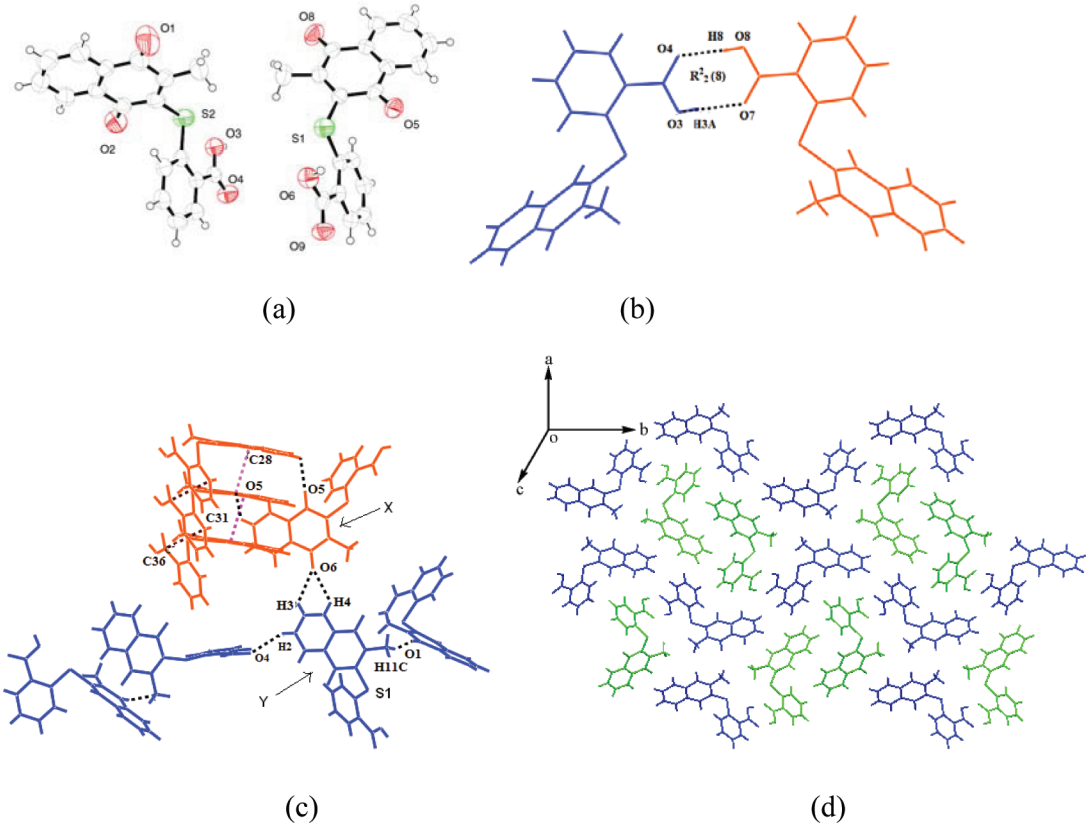

Figure 5. (a) ORTEP diagram of polymorph **III** (50% thermal ellipsoids). (b) The arrangement of symmetry independent molecules in lattice (**X** red and **Y** blue). (c) Weak interaction among molecules of polymorph **III.** (d) Packing diagram of **III** embracing of two molecules of one type of symmetry by six molecules of another type.

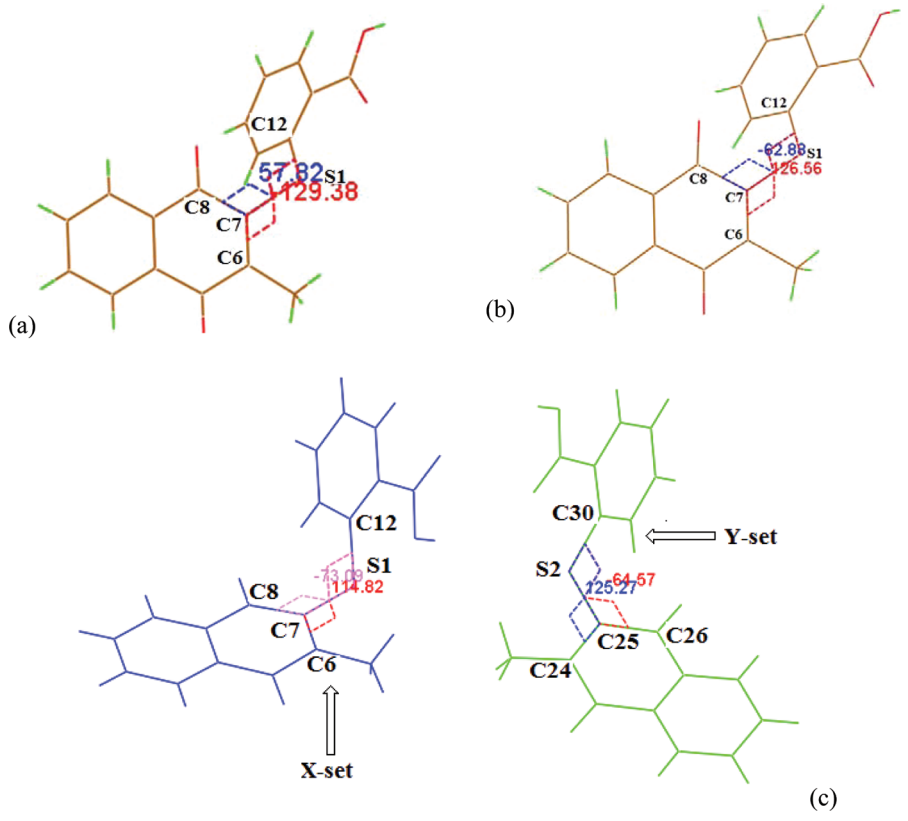

Figure 6. Torsion angles of polymorph (a) **I**, (b) **II**, (c) **III** showing the orientation of the thiosalicylic acid part with respect to the 2-methyl 1,4-naphthoquinone part.

dx.doi.org/10.1021/cg300318u | *Cryst. Growth Des.* 2012, 12, 3114−3122

Crystallization of 2-(1,4-dihydro-1,4-dioxonaphthalen-3-ylthio)benzoic acid **L** from different solvents such as THF/acetone, methanol, and chloroform led to three different polymorphs **I**–**III**. Polymorph **I** crystallizes in triclinic space group $P\bar{1}$ from a solution **L** in mixed solvents of THF and acetone. In its crystal structure (Figure 3a), it is observed that the sulfur atom bearing 2-methyl 1,4-naphthoquinone groups are trans to each other across a $R^2_2(8)$ type of cyclic hydrogen bond motif (Figure 3b). The carboxylic acid groups exhibit strong O4–H4A···O3 interactions and form a cyclic hydrogen bond architecture as shown in Figure 3b. Polymorph **I** forms a layered 1D polymeric structure in the lattice through C–H···O (Table 1) interactions. Interestingly, polymorph **I** exhibits strong C18–O3···S1 interactions in its lattice. The polymorph **I** also shows $\pi\cdots\pi$ interactions between the phenyl moiety and the carboxylic acid group containing a carbon atom with a distance $C13_{Phenyl}\cdots C18_{carboxy}$ 3.379 Å as shown in Figure 3c.

Table 2. Torsion Angles of Polymorphs I–III

polymorph	dihedral angles
I	C6–C7–S1–C12, −129.38°; C8–C7–S1–C12, 57.82°
II	C6–C7–S1–C12, 126.56°; C8–C7–S1–C12, −62.88°
III	For X-set: C6–C7–S1–C12, 114.82°; C8–C7–S1–C12, −73.09°.
	For Y-set: C24–C25–S2–C30, 125.27°; C26–C25–S2–C30, −64.57°.

Polymorph **II** crystallizes in monoclinic space group $P2_1/c$ from a solution of **L** in methanol. The ORTEP diagram of the polymorph **II** is shown in Figure 4a. Crystal packing of the polymorph **II** shows that the carboxylic acids are engaged in strong O4–H4···O3 interactions. Such interactions lead to the

Table 3. Hydrogen Bond Geometries (Å, °) for Solvate IV and Cocrystal V

solvate/cocrystal	D–H···A	d_{D-H}	$d_{H\cdots A}$	$d_{D\cdots A}$	∠D–H···A
IV	O7–H7···O10	0.82	1.86	2.68(3)	177.3
	O9 –H9···O8	0.82	1.85	2.66(3)	172.9
	O11–H11···O12 [−x, 1 − y, −z]	0.82	1.80	2.61(3)	173.9
	C11–H11A···S1	0.96	2.70	3.13(4)	108.5
	C29–H29C···S2	0.96	2.68	3.15(4)	111.6
	C34 –H34···O9	0.93	2.34	2.68(4)	101.5
	C47– H47C···S3	0.96	2.64	3.13(3)	113.1
	C49–H49···O2 [x, −1 + y, z]	0.93	2.43	3.23(4)	144.9
	C56 –H56···O1 [−1 + x, y, z]	0.96	2.33	3.15(5)	142.8
	C56–H56···O4 [1 − x, 1 − y, 1 − z]	0.96	2.31	3.25(5)	167.5
V	C11–H11B···S1	0.96	2.69	3.09	106.6
	C13–H13···O3 [−1 + x, y, z]	0.93	2.53	3.42	161.7
	C16–H16···O2	0.93	2.37	2.70	101.1
	C19–H19···O1	0.93	2.47	3.25	141.4
	C20–H20···O1 [1 − x, 1 − y, 1 − z]	0.93	2.60	3.49	164.1
	C23–H23···O2	0.93	1.87	2.76	167.1
	C23–H23···N1 [1 − x, −y, 1 − z]	0.93	2.48	2.83	103.0

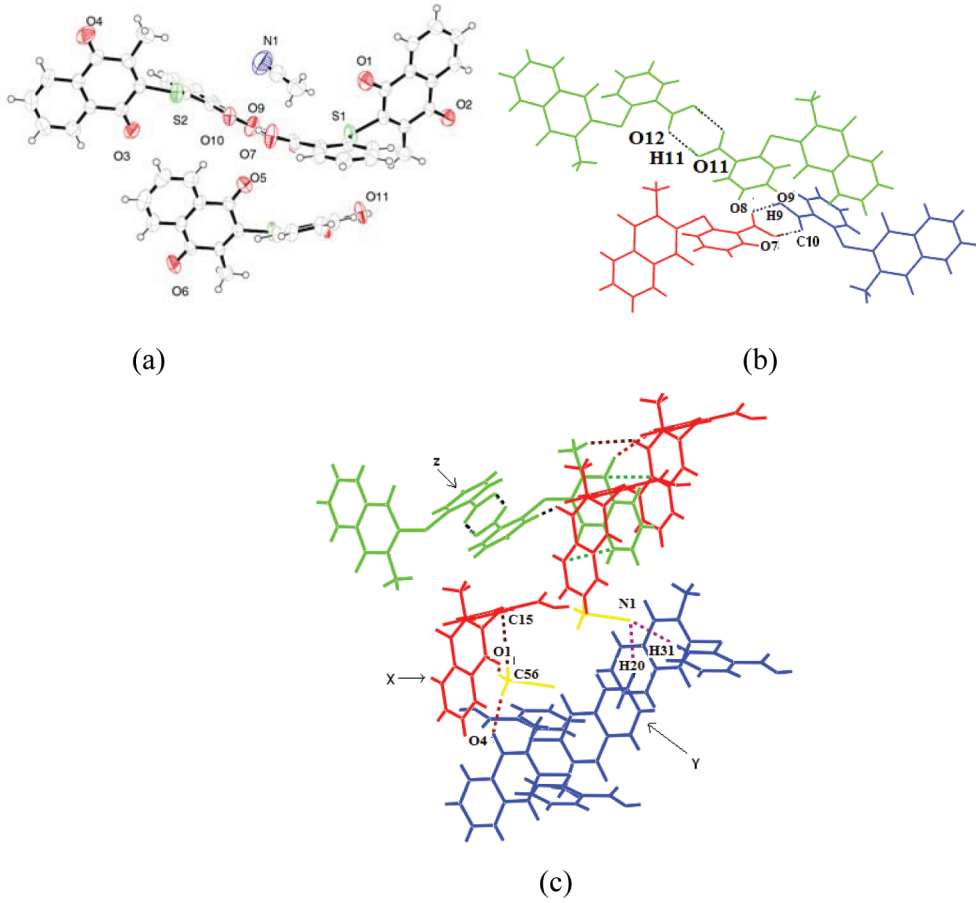

Figure 7. (a) ORTEP diagram of **IV** (drawn with 50% thermal ellipsoids). (b) The H-bond interactions to form dimeric assemblies among symmetry independent molecules. (c) Weak interactions contributing to self-assembly formation in **IV**.

dx.doi.org/10.1021/cg300318u | *Cryst. Growth Des.* 2012, 12, 3114–3122

formation of cyclic hydrogen bond architectures as shown in Figure 4b. The packing pattern of the polymorph **II** is guided by C16−H16···O1 and C2−H2···O2 interactions (Table 1). These overall weak interactions help in generating a 1D polymeric structure. Besides that, the structure of polymorph **II** extends to a 1D zigzag architectures by strong $\pi\cdots\pi$ interactions of the phenyl moiety with the carbon atom of the carboxylic acid group ($C13_{Phenyl}\cdots C18_{carboxy}$ 3.34 Å) as shown in Figure 4c.

The polymorph **III** is obtained from a solution of **L** in chloroform; it crystallizes in orthorhombic space group $P2_12_12_1$. The structure of the polymorph **III** is shown in Figure 5a. Polymorph **III** has two symmetry independent molecules (X and Y) in the crystallographic asymmetric unit as shown in Figure 5b. From the crystal lattice, it is observed that sulfur atom bearing 2-methyl 1,4-naphthoquinone groups are cis to each other across $R^2_2(8)$ types of cyclic hydrogen bond motif architectures as shown in Figure 5b. Both the molecules exhibit strong O3−H3A···O7 and O8−H8···O4 (Table 1) interactions, leading to formation of a cyclic hydrogen bond architecture. It is observed that polymorph **III** assembles in the lattice through C20−H20···O5 interactions. Oxygen atoms on quinones are involved in bifurcated C3−H3···O6 and C4−H4···O6 interactions to form a 1D linear architecture as shown in Figure 5c. Besides that polymorph **III** adopts a 1D layered structure by strong $\pi\cdots\pi$ interactions between phenyl moieties with the carboxylic acid groups. The packing diagram of the molecules shown in Figure 5d indicates that there are pair of molecules of one type of symmetry get embraced by six molecules that have another type of symmetry. If we compare the packing pattern of polymorph **I** one can see an arrangement of head−head (Figure 3d), whereas in polymorph **II** has head to tail arrangements (Figure 4d). These make the lattice of these three polymorphs clearly distinguishable.

From these structures, it is observed that the torsion angle of C8−C7−S1−C12 and C6−C7−S1−C12 of polymorph **II** are −62.88°, 126.56°, whereas in polymorph **I** the torsion angles of C8−C7−S1−C12 and C6−C7−S1−C12 are 57.82° and −129.38° (Figure 6), respectively, which shows the difference between the conformation of the polymorphs **I** and **II**. Both symmetry independent molecules of the polymorph **III** (X and Y) show different torsion angles. The torsion angle for X-set, namely, C8−C7−S1−C12, C6−C7−S1−C12 are −73.09° and 114.82°, respectively, whereas torsion angles of C26−C25−S2−C30, C24−C25−S2−C30 for molecules designated as Y-set are −64.57° and 125.27°, respectively. The torsion angles are shown in Table 2.

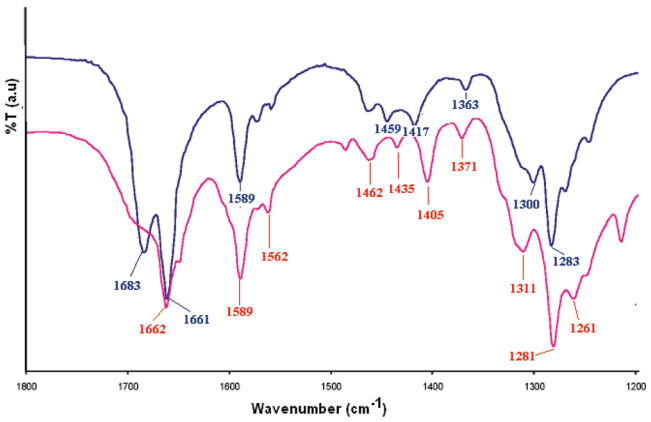

Figure 8. Solid state IR (KBr, cm^{-1}) spectra of in the region of 1800−1200 cm^{-1} of polymorph **I** (top, blue line) and cocrystal **V** (bottom, red line).

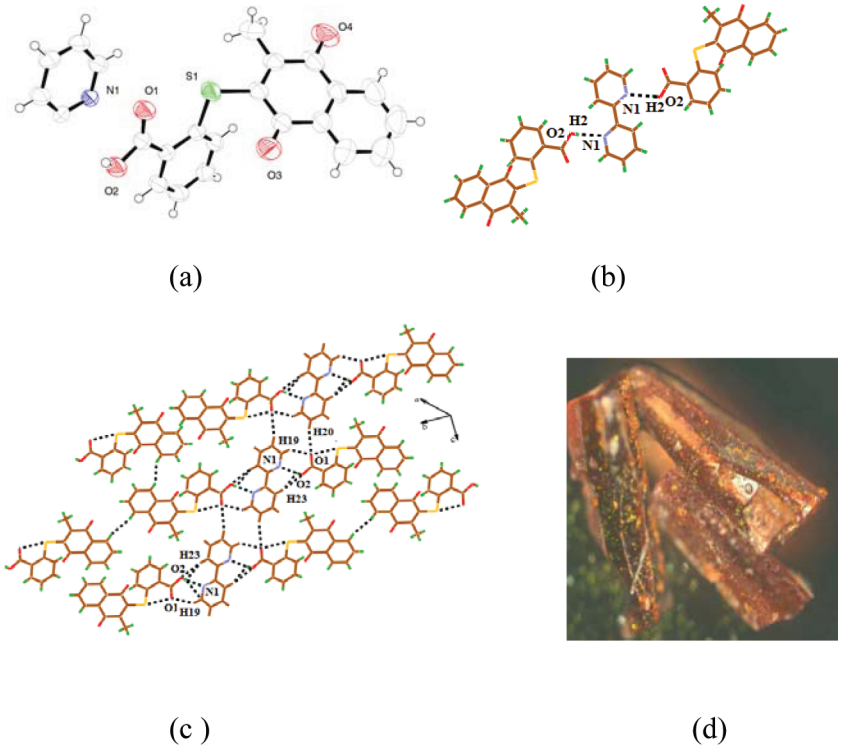

Figure 9. (a) Asymmetric unit of the cocrystal **V**. (b) O−H···N interactions in **V**. (c) Weak interactions in crystal lattice of **V**. (d) Crystal morphology of **V**.

dx.doi.org/10.1021/cg300318u | *Cryst. Growth Des.* 2012, 12, 3114−3122

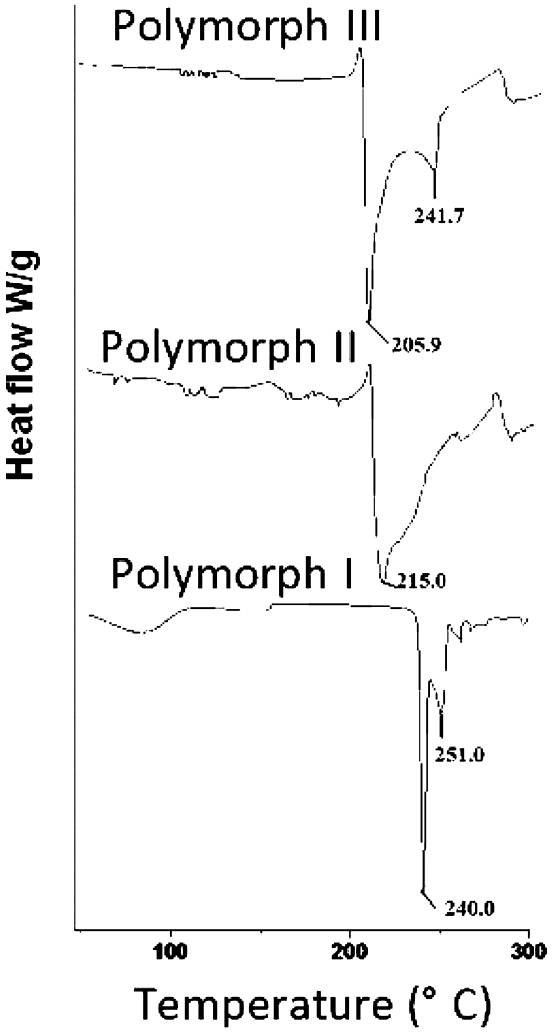

Figure 10. Differential scanning calorimetry of polymorph **I**–**III** (heating rate 5 °C per minute).

The structures containing more than one molecule in the crystallographic asymmetric unit are suggested to be important for close inspection of the reaction coordinate of supramolecular reactions.[14a] There are good numbers of examples of polymorphic systems that have multiple Z′.[14] In the present polymophs **I**–**III**, we can clearly see a very close correlation between the structures; namely, structures of **I** and **III** are analogous to regio-isomers in organic chemistry. In this case, the positions of the substituents across a rigid functionality formed by supramolecular interactions (dimeric carboxylic acid part) cause the differences in these structures, whereas polymorphs **I** and **II** have slight orientation differences in the position of the rings across the cyclic dimeric H-bonded motifs. This is revealed in the torsion angle between the two aromatic rings present in these polymorphs. The torsion angles between the aromatic ring and 2-methyl 1,4-naphthoquinone ring in **I** and **II** are −57.04° and 126.56°, respectively.

It is interesting to know while formation of the solvates the original packing pattern of any of the polymorphs and the weak interaction patterns of the polymorphs are retained in them or not. Thus we have studied the structure of an acetonitrile solvate of **L** and a cocrystal of 2,2′-bipyridine with **L**. Solvate **IV** crystallizes in triclinic space group $P\bar{1}$. The crystal structure of the **IV** is shown in Figure 7a. It has three symmetry independent molecules of **L** (X, Y, and Z) with one solvate molecule (acetonitrile) in the crystallographic asymmetric unit (Figure 7a). In solvate **IV**, among the three symmetry independent **L**, two of them, namely, the X and Y-set of molecules, are engaged in $R^2_2(8)$ type of cyclic hydrogen bond motif, whereas the Z-set of molecules leads to the formation of a cyclic hydrogen bonding architecture among themselves (Figure 7b). The hydrogen bond parameters are listed in Table 3. Thus, the dimeric hydrogen bonds are not broken by acetonitrile as guest molecules. It is observed that sulfur atoms bearing 2-methyl 1,4-naphthoquinone groups are trans to each other. From the crystal lattice, it is observed that solvate **IV** assembles through C−H···O interactions between the quinonic moieties and solvent molecules. This leads to the formation of a 1D zigzag supramolecular polymeric structure.

Interestingly, the N atom of acetonitrile molecules exhibits bifurcated C20−H20···N1 and C31−H31···N1 interactions (Figure 7c). The solvate **IV** has an extended 1D layer supported by strong lateral $\pi\cdots\pi$ interactions between phenyl moieties with the carboxylic acid groups.

There are possibilities of formation of salt as well as cocrystal of **L** with 2,2′-bipyridine. But when the compound **L** was reacted with with 2,2′-bipyridine, we observed cocrystal formation between them. The evidence comes from the IR spectra of the cocrystal with compound **L**. For clarity if one looks at the IR spectra of the cocrystal **V** and compares it with the IR spectra of **L** (Figure 8), it is observed that the signature of the carbonyl stretching of carboxylic acid at 1683 cm^{-1} is retained in the cocrystal **V**. However, there is broadening occurring due to additional peaks from cocrystal **V**. A salt formation would have changed the position of this peak significantly supporting the cocrystal formation in this case. Further, the O−H stretching of the **L** and the cocrystals **V** have a very close resemblance; these stretching frequencies appear as broad signals at 3444 cm^{-1} and 3452 cm^{-1}, respectively (Supporting Information), confirming the identity of **V** as a cocrystal.

A 2:1 cocrystal of **L** with 2,2′-bipyridine, **V** crystallizes in triclinic space group $P\bar{1}$. The asymmetric unit of the cocrystal comprises one **L** along with the half of the 2,2′-bipyridine molecule (Figure 9a). The 2,2′-bipyridine acts as a bridge between the two carboxylic acid molecules. The two nitrogen atoms are hydrogen bonded to carboxylic acids through O2−H2···N1 interactions as shown Figure 9b. The nitrogen atoms of the 2,2′-bipyridine are in a trans-disposition across the C−C connecting the two rings. There are very weak C−H···O (Table 3) interactions to provide rigidity to the assembly as shown in Figure 9c. Participation of the C−H bond present at the ortho-position of an aromatic ring is commonly encountered in cocrystals of carboxylic acid with pyridine or quinoline molecules.[15] The 2,2′-bipyridine molecules are found to be intercalated in the layers between the carboxylic acid molecules, thereby making a sheetlike intercalated structure. It may be mentioned that 4,4′-bipyridine forms salts with different aromatic dithio aromatic acids,[15a] and in such cases the proton transfer takes place to form ionic type of interactions. In our case, we observe trans geometry of the 2,2′-bipyridine molecule which is present in the parent molecule,[16] and this shows that even though there is possibility to adopt a cis-geometry through the two nitrogen atoms via bifurcated hydrogen bonding to acidic hydrogen atom it prefers to retain its original geometry. This makes a distinction on conformation of 2,2′-bipyridine in a supramolecular and coordination environments; in the latter case the *cis*-geometry to form chelate is preferred.

dx.doi.org/10.1021/cg300318u | *Cryst. Growth Des.* 2012, 12, 3114–3122

Table 4. Crystallographic Parameters of I–V

compound no.	I	II	III	IV	V
formulas	$C_{18}H_{12}O_4S$	$C_{18}H_{12}O_4S$	$C_{18}H_{12}O_4S$	$C_{56}H_{39}NO_{12}S_3$	$C_{23}H_{16}NO_4S$
formula wt	324.25	324.25	324.25	1014.09	402.44
crystal system	triclinic	monoclinic	orthorhombic	triclinic	triclinic
space group	$P\bar{1}$	$P2_1/c$	$P2_12_12_1$	$P\bar{1}$	$P\bar{1}$
a (Å)	4.78 (4)	4.941(2)	4.903(3)	7.7394(3)	5.0244 (3)
b (Å)	7.93 (5)	10.113(5)	22.146(12)	13.4693(6)	9.5728 (6)
C (Å)	20.85 (15)	30.621(14)	27.486(14)	24.0125(12)	19.9981 (13)
α (°)	89.02	90.00	90.00	103.506(12)	82.573 (5)
β (°)	83.94	93.72 (3)	90.00	99.067(3)	84.043 (4)
γ (°)	73.13	90.00	90.00	96.329(3)	85.488 (5)
V (Å^3)	752.43 (10)	1527.0(12)	2985.0(3)	2375.18(18)	946.56 (10)
Z	2	4	8	2	2
density/Mg m^{-3}	1.432	1.411	1.444	1.418	1.412
abs coeff /mm^{-1}	0.233	0.230	0.235	0.225	0.202
F(000)	336	672	1344	1052	418
total no. of reflections	7534	6844	26663	25441	4344
reflections, $I > 2\sigma(I)$	1635	1822	2486	5286	4318
max 2θ/°	50.00	49.66	50.00	48.46	54.90
ranges (h, k, l)	$-5 \le h \le 5$	$-5 \le h \le 5$	$-5 \le h \le 5$	$-8 \le h \le 8$	$-6 \le h \le 6$
	$-9 \le k \le 9$	$-11 \le k \le 11$	$-26 \le k \le 26$	$-15 \le k \le 15$	$-12 \le k \le 12$
	$-24 \le l \le 24$	$-36 \le l \le 36$	$-33 \le l \le 33$	$-27 \le l \le 27$	$-25 \le l \le 25$
complete to 2θ (%)	100.0	98.6	100.0	95.8	100.0
data/restraints/parameters	2666/0/210	2596/0/210	3160/0/419	7652/0/656	4344/0/263
GOF (F^2)	1.161	1.091	1.044	1.007	0.954
R indices [$I > 2\sigma(I)$]	0.0330	0.1023	0.0296	0.0452	0.0492
R indices (all data)	0.0431	0.2140	0.0357	0.0697	0.0493

Powder X-ray diffraction (PXRD) patterns of the samples whose structures are presented can be indexed and comparable to their respective simulated PXRD patterns to a satisfactory extent (Supporting Information); there are few unassigned peaks especially in the case of polymorph **2**. So, we have recorded the PXRD of the thiosalicylic acid to see if any amount is present in it as an impurity (please see Supporting Information). Comparing the PXRD of thisalicylic acid with the PXRD of polymorph **II**, matching was not observed; thus, the additional peaks encountered in the case of **II** may be attributed to the phase impurity during crystallization. Differential scanning calorimetry analyses show endothermic peaks in the cases of **I–V**.

The differential scanning calorimetry has been one of the key methods to identify the monotropic and enantiotropic systems,[17] and these are guided by Burger and Ramberger rules;[17b] however, in our DSC the plots of each of **I–III** are independent of each other and common endothermic processes as well as reversibility on cooling are not observed in our case. DSC profiles of the polymorphs **I–III** have clear distinctions and are shown in Figure 10. Endothermic processes at 240 and 251 °C for **I**; 215.0 °C for **II**; at 205.9 °C and at 241.7 °C for **III** respectively are observed. These corresponding to melting points followed by phase transition are thus characteristic of the polymorphs and clearly indicate the difference in packing patterns in the solid state.

In summary, three conformational polymorphs of 2-(1, 4-dihydro-1,4-dioxonaphthalen-3-ylthio) benzoic acid are demonstrated. In each polymorph, the dimeric forms of carboxylic acids are observed. Because of the orientation of the aromatic groups across a hydrogen bond motif, different polymorphs **I–III** are formed. Similar conformational polymorphs arise in fuchsones,[9] but in this study we have tailor-made the effect of formation of dimeric assemblies by carboxylic acid functional group of the quinone tethered carboxylic acid to stabilize such conformational changes across a supramolecular motif to observe polymorphs. The weak interactions associated with the substituent on quinone rings helps in stabilizing different supramolecular structures. The salvation, as in the case of solvate **IV** and cocrystals formation, as in the case of **V**, can lead to either retention or disruption of hydrogen bonded dimeric assemblies of carboxylic acid units.

EXPERIMENTAL SECTION

2-(1,4-Dihydro-2-methyl-1,4-dioxonaphthalen-3-ylthio)-benzoic acid (L). A solution of 2-methyl-1,4-naphthoquinone (0.34 g, 2 mmol), thiosalicylic acid (0.30 g, 2 mmol) in methanol (20 mL) was stirred for 3 h at room temperature. The color of the reaction mixture slowly turned yellow followed by formation of yellow precipitate. The precipitate was collected by filtration and dried in open air. Yield: 95%. IR (KBr, cm^{-1}): 3444 (m), 2922 (w), 2846 (w), 1683 (m), 1661 (s), 1589 (m), 1459 (w), 1417 (s), 1300 (m), 1283 (s), 1179 (w), 1035 (m), 955 (m), 842 (w), 787 (w), 741 (w), 710 (w), 650 (w). ^{1}HNMR (400 MHz, DMSO-d_6): 8.06 (d, J = 7.2 Hz, 1H), 7.92 (dd, J = 2.4 Hz, 1H), 7.85 (dd, J = 2.4 Hz, 1H), 7.83 (d, J = 7.2 Hz, 1H,), 7.32 (d, J = 6.0 Hz,1H), 7.29 (dd, J = 7.2 Hz, 2H), 7.23 (d, J = 6.0 Hz, 1H) 2.34 (s, 3H). ^{13}C NMR (DMSO-d_6): 182.7, 180.0, 167.5, 152.8, 142.5, 138.4, 134.1, 134.0, 132.4, 132.1, 132.0, 130.9, 128.9, 128.3, 126.5, 126.3, 125.3, 16.0.

Polymorph I. The polymorph **I** was obtained from a solution of **L** in THF/acetone (1:1v ratio) after 7 days (yield >90%). IR (KBr, cm^{-1}): 3444 (m), 2922 (w), 2846 (w), 1683 (m), 1661 (s), 1589 (m), 1459 (w), 1417 (s), 1300 (m), 1283 (s), 1179 (w), 1035 (m), 955 (m), 842 (w), 787 (w), 741 (w), 710 (w), 650 (w).

Polymorph II. The polymorph **II** was crystallized as red block from a solution of **L** in methanol after 3 days (yield >40%).

Polymorph III. The polymorph **III** was obtained from a solution of **L** in chloroform after 4 h (yield >70%).

Solvate IV. The solvate **IV** was obtained as yellow crystals from a solution of **L** in acetonitrile after one week (yield ~65%).

dx.doi.org/10.1021/cg300318u | Cryst. Growth Des. 2012, 12, 3114–3122

Cocrystal V. A methanolic solution of 1:1 mixture of 2-(1,4-dihydro-1,4-dioxonaphthalen-3ylthio)benzoic acid and 2,2′-bipyridyl was kept undisturbed for crystallization. Yellow crystals were obtained after a day. Yield: > 40% with respect to **L**. IR (KBr, cm^{-1}): 3452 (bw), 3061 (w), 2922 (m), 2851 (w), 2432 (w), 1662 (s), 1589 (s), 1562 (m), 1462 (w),1435 (m), 1405 (m), 1371 (m), 1311 (w), 1281 (m), 1261 (m), 1214 (w), 1057 (w), 799 (m), 746 (w), 707 (w), 627 (w), 619 (w).

The X-ray single crystal diffraction data were collected at 296 K with Mo Kα radiation (λ = 0.71073 Å) using a Bruker Nonius SMART CCD diffractometer equipped with a graphite monochromator. The SMART software was used for data collection and also for indexing the reflections and determining the unit cell parameters; the collected data were integrated using SAINT software. The structures were solved by direct methods and refined by full-matrix least-squares calculations using SHELXTL software.[18] All the non-H atoms were refined in the anisotropic approximation against F^2 of all reflections. The H-atoms, except those attached to oxygen atoms, were placed at their calculated positions and refined in the isotropic approximation; those attached to oxygen were located in the difference Fourier maps and refined with isotropic displacement coefficients. The crystallographic parameters of the compounds are tabulated in Table 4.

■ ASSOCIATED CONTENT

Ⓢ Supporting Information

CIF files, powder XRD of **I**−**V** are available. These materials are available free of charge via the Internet at http://pubs.acs.org.

■ AUTHOR INFORMATION

Corresponding Author

*E-mail: juba@iitg.ernet.in.

Notes

The authors declare no competing financial interest.

■ ACKNOWLEDGMENTS

The authors thank Council of Scientific and Industrial Research (New Delhi) India for financial assistance.

■ REFERENCES

(1) (a) Bernstein, J. *Polymorphism in Molecular Crystals*; Clarendon: Oxford, 2002. (b) McCrone, W. C. In *Physics and Chemistry of the Organic Solid State*; Fox, D.; Labes, M. M.; Weissberger, A., Eds.; Wiley-Interscience: New York, 1965; Vol. *2*, p 726. (c) Braga, D.; Grepioni, F. *Chem. Soc. Rev.* **2000**, *29*, 229−238. (d) Threlfall, T. L. *Analyst* **1995**, *120*, 2435−2460. (e) Bilton, C.; Howard, J. A. K.; Madhavi, N. N. L.; Nangia, A.; Desiraju, G. R.; Allen, F. H.; Wilson, C. C. *Chem. Commun.* **1999**, 1675−1676. (f) Zhang, H. Y.; Zhang, Z. L.; Zhang, J. Y.; Ye, K. Q.; Gao, H. Z.; Wang, Y. *CrystEngComm* **2007**, *9*, 951−958. (g) Tamura, R.; Iwama, S.; Gonnade, R. G. *CrystEngComm* **2011**, *13*, 5269−5280. (h) Ma, Z.; Moulton, B. *J. Chem. Crystallogr.* **2009**, *39*, 913−918.

(2) (a) Sarma, R. J.; Baruah, J. B. *Chem.—Eur. J.* **2006**, *12*, 4994−5000. (b) Dey, A.; Desiraju, G. R. *CrystEngComm* **2006**, *8*, 477−481.

(3) (a) Desiraju, G. R.; Paul, I. C.; Curtin, D. Y. *J. Am. Chem. Soc.* **1977**, *99*, 1594−1601. (b) Bernstein, J.; Davey, R. J.; Henck, J. O. *Angew. Chem., Int. Ed.* **1999**, *38*, 3440−3461. (c) Greer, M. L.; McGee, B. J.; Rogers, R. D.; Blackstock, S. C. *Angew. Chem., Int. Ed.* **1997**, *36*, 1864−1866. (d) Byrn, S. R., *Solid State Chemistry of Drugs*; Academic Press: New York, 1982. (e) DeCamp, W. H. In *Crystal Growth of Organic Materials*; Myerson, A. S.; Green, D. A.; Meenan, P., Eds.; ACS Proceedings Series: *American Chemical Society*: Washington, DC, 1996. (f) Dunitz, J. D.; Bernstein, J. *Acc. Chem. Res.* **1995**, *28*, 193−200. (g) Desiraju, G. R. *Nat. Mater.* **2002**, *1*, 77−79. (h) Nangia, A.; Desiraju, G. R. *Chem. Commun.* **1999**, 605−606. (i) Laird, T. *Org. Process Res. Dev.* **2000**, *4*, 371−379. (j) Rogers, R. D. *Cryst. Growth Des.* **2003**, *3*, 867.

(4) (a) Long, S.; Parkin, S.; Siegler, M. A.; Cammers, A.; Li, T. *Cryst. Growth Des.* **2008**, *8*, 4006−4013. (b) Nangia, A. *Acc. Chem. Res.* **2008**, *41*, 595−604. (c) Desiraju, G. R. *Acc. Chem. Res.* **1996**, *29*, 441−449. (d) Desiraju, G. R. *Acc. Chem. Res.* **2002**, *35*, 565−573.

(5) (a) Desiraju, G. R. *Angew. Chem., Int. Ed.* **1995**, *34*, 2311−2327. (b) Bilton, C.; Howard, J. A. K.; Madhavi, N. N. L.; Nangia, A.; Desiraju, G. R.; Allen, F. H.; Wilson, C. C. *Chem. Commun.* **1999**, 1675−1676. (c) Kumar, V. S. S.; Addlagatta, A.; Nangia, A.; Robinson, A.; Broder, W. T.; Mondal, C. K.; Evans, I. R.; Howard, J. A. K.; Allen, F. H. *Angew. Chem., Int. Ed.* **2002**, *41*, 3848−3851. (d) Chen, S.; Guzei, I. A.; Yu, L. *J. Am. Chem. Soc.* **2005**, *127*, 9881−9885.

(6) (a) *Polymorphism in Pharmaceutical Solids*; Brittain, H. G., Ed.; Marcel Dekker: New York, 1999. (b) Vishweshwar, P.; McMahon, J. A.; Oliveira, M.; Peterson, M. L.; Zaworotko, M. J. *J. Am. Chem. Soc.* **2005**, *127*, 16802−16803. (c) Fabbiania, F. P. A.; Allan, D. R.; Parsons, S.; Pulham, C. R. *CrystEngComm* **2005**, *7*, 179−186.

(7) (a) Jali, B. R.; Singh, W. M.; Baruah, J. B. *CrystEngComm* **2011**, *13*, 763−767. (b) Singh, W. M.; Baruah, J. B. *J. Mol. Struct.* **2009**, *931*, 82−86. (c) Kashyap, R. P.; Sun, D.; Watson, W. H. *J. Chem. Crystallogr.* **1995**, *25*, 339−349.

(8) (a) Kinuta, T.; Sato, T.; Tajima, N.; Matsubara, Y.; Miyazawa, M.; Imai, Y. *CrystEngComm* **2012**, *14*, 1016−1020. (b) Imai, Y.; Kinuta, T.; Nagasaki, K.; Harada, T.; Sato, T.; Tajima, N.; Sasaki, Y.; Kuroda, R.; Matsubara, Y. *CrystEngComm* **2009**, *11*, 1223−1226.

(9) (a) Chandran, S. K.; Nath, N. K.; Roy, S.; Nangia, A. *Cryst. Growth Des.* **2008**, *8*, 140−154. (b) Nath, N. K.; Nilapwar, S.; Nangia, A. *Cryst. Growth Des.* **2012**, *12*, 1613−1625.

(10) (a) Desiraju, G. R. *Angew. Chem., Int. Ed.* **2007**, *46*, 8342−8356. (b) Desiraju, G. R. *CrystEngComm* **2007**, *9*, 91−92.

(11) (a) Goldberg, L.; Ocherashvilli, A.; Daniels, D.; Last, D.; Cohen, Z. R.; Tamar, G.; Kloog, Y.; Mardor, Y. *Mol. Cancer Ther.* **2008**, *7*, 3609−3616. (b) Halaschek-Wiener, J.; Kloog, Y.; Wacheck, V.; Jansen, B. *J. Invest. Dermatol.* **2003**, *120*, 1−7. (c) Smalley, K. S.M.; Eisen, T. G. *Int. J. Cancer* **2002**, *98*, 514−522. (d) Ozkay, U. D.; Ozkay, Y.; Can, O. D. *Med. Chem. Res.* **2011**, *20*, 152−157.

(12) Rane, S.; Ahmed, K.; Salunke-Gawali, S.; Zaware, S. B.; Srinivas, D.; Gonnade, R.; Bhadbhade, M. *J. Mol. Struct.* **2008**, *892*, 74−83.

(13) Singh, W. M.; Baruah, J. B. *Syn. Commun.* **2009**, *39*, 1433−1442.

(14) (a) Desiraju, G. R. *CrystEngComm* **2007**, *9*, 91−92. (b) Steed, J. W. *CrystEngComm* **2003**, *5*, 169−179. (c) Aitipamula, S.; Nangia, A. *Chem.—Eur. J.* **2005**, *11*, 6727−6742. (d) Chandran, S. K.; Nangia, A. *CrystEngComm* **2006**, *8*, 581−585. (e) Hao, X.; Siegler, M. A.; Perkin, S.; Brock, C. P. *Cryst. Growth Des.* **2005**, *5*, 2225−2232. (f) Das, D.; Banerjee, R.; Mondal, R.; Howard, J. A. K.; Boese, R.; Desiraju, G. R. *Chem. Commun.* **2006**, 555−557. (g) Baruah, J. B.; Karmakar, A.; Barooah, N. *CrystEngComm* **2008**, *10*, 151−154. (h) Brock, C. P.; Duncan, L. L. *Chem. Mater.* **1994**, *6*, 1307−1312. (i) Steed, J. W.; Sakellararious, E.; Junk, P. C.; Smith, M. K. *Chem.—Eur. J.* **2001**, *7*, 1240−1247. (j) Long, S.; Siegler, M. A.; Mattei, A.; Li, T. *Cryst. Growth Des.* **2011**, *11*, 414−421.

(15) (a) Broker, G. A.; Tiekink, E. R. T. *CrystEngComm* **2007**, *9*, 1096−1109. (b) Arman, H. D.; Kaulgud, T.; Tieknik, E. R. T. *Acta Crystallogr.* **2010**, *E66*, o2602.

(16) Merritt, L. L.; Schroeder, E. *Acta Crystallogr.* **1956**, *9*, 801−804.

(17) (a) Rodriguez-Spong, B.; Price, C. P.; Jayasankar, A.; Matzer, A. J.; Rodriguez-Hornedo, N. *Adv. Drug Delivery Rev.* **2004**, *56*, 241−274. (b) Burger, A.; Ramberger, R. *Mikrochim. Acta* **1979**, *2*, 259−279. (c) Kawakami, K. *J. Pharm. Sci.* **2007**, *96*, 982−989.

(18) Sheldrick, G. M. *Acta Crystallogr.* **2008**, *A64*, 112−122.